

## Metadata of the chapter that will be visualized online

---

Chapter Title	Thermal Hysteresis
Copyright Year	2020
Copyright Holder	Springer Nature Switzerland AG
Corresponding Author	Family Name <b>Kristiansen</b> Particle Given Name <b>Erlend</b> Suffix Organization NTNU University Library Address Trondheim, Norway Email erlendkr@ntnu.no

---

Abstract	Antifreeze (glyco)proteins, AF(G)Ps, are defined by their shared ability to prevent ice crystals from growing in supercooled solutions. They are categorized as being either moderately active or hyperactive. The distinct difference in antifreeze potency between these two categories is accompanied by distinct shapes of the ice crystals that are being stabilized in their presence; moderately active AF(G)Ps cause bipyramidal crystals to develop, a shape that only exposes a single crystal plane to the surrounding solution. In the presence of hyperactive AF(G)Ps, ice crystals express several crystal planes. A number of different factors affect their potency as antifreeze agents, from large organic macromolecules to inorganic ions. This chapter outlines current understanding of the modus operandi of AF(G)Ps. Attempts are made to provide some simple explanations to the antifreeze potency of AF(G)Ps, including their characteristics as moderately active or hyperactive, and how their antifreeze potency is affected by different factors. The different potencies of moderately and hyperactive AF(G)Ps are ascribed to differences in their adsorption habits. Effects of additives or molecular size on their potencies are ascribed to variations in protein solubility, induced by variations in molecular size or evoked by the presence of additives. Experimental proof of concept is discussed in the context of basic solubility theory. Some characteristics of ice-nucleating agents (INAs) in relation to AF(G)Ps and their relevance in cold tolerance is also briefly examined.
----------	--

---

Keywords (separated by ‘-’)	Thermal hysteresis - Antifreeze activity - Kelvin effect - Critical radius - Hyperactive - Hyperactivity - Protein size - Protein solubility - Hofmeister series - Additive - Enhancement - Adsorption - Desorption - Heterogeneous nucleation - Ice nucleator - Ice nucleating agent
--------------------------------	---

---

# Chapter 6 1

## Thermal Hysteresis 2

Erlend Kristiansen 3

### 6.1 Introduction

Thermal hysteresis refers to the phenomenon where antifreeze proteins (AFPs) or antifreeze glycoproteins (AFGPs) cause a separation of the freezing and melting temperature of existing ice crystals in solution. This ability to separate the melting and freezing temperature of ice is limited in that on sufficient cooling the ice crystal undergoes a sudden and rapid ice growth. Ramsay (1964) when studying a mechanism of water reabsorption in the beetle *Tenebrio molitor* first reported the phenomenon. In a footnote, he states: 10

When small ice crystals are observed under the microscope, as in the freezing-point method of Ramsay and Brown, one notices that large crystals grow at the expense of small ones and that the edges of the crystals are rounded—the natural consequences of surface tension at the water-ice interface. The change of state between solid and liquid is perfectly temperature-reversible. . . . By contrast, the crystals which appear in fluid from the anterior perinephric space tend to have jagged outline and large crystals do not grow at the expense of smaller ones. Furthermore, the system is not temperature-reversible. As the temperature is raised the crystals decrease in size, but as the temperature is lowered they do not increase in size. After the temperature has been lowered by a few degrees the crystal suddenly begins to grow rapidly. On occasion undercooling of the order of 10 °C was observed (in the continued presence of small crystals) and then suddenly the whole sample appeared to solidify instantaneously. 22

The temperature interval between the melting and freezing temperatures is referred to as the hysteresis gap, and the lower temperature where rapid ice growth is initiated is termed the hysteresis freezing point. The quantitative difference between the melting temperature and the hysteresis freezing point is termed the hysteresis activity, or antifreeze activity. 27

---

E. Kristiansen (✉)  
 NTNU University Library, Trondheim, Norway  
 e-mail: [erlendkr@ntnu.no](mailto:erlendkr@ntnu.no)

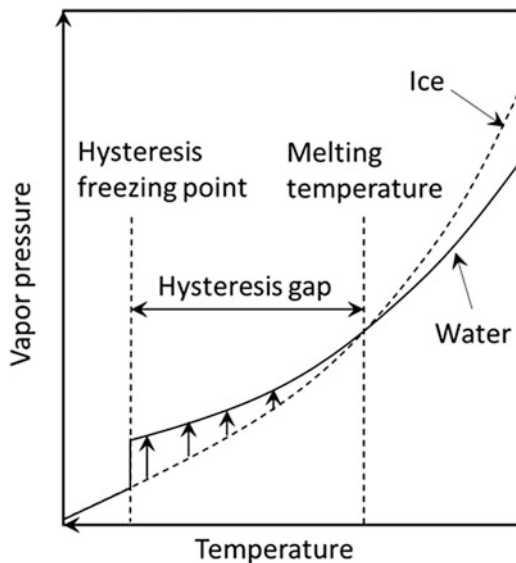
28 Thermal hysteresis reflects the role of AF(G)Ps as protectors against ice nucle-  
29 ation in the supercooled body fluids of freeze avoiding animals. Their presence  
30 enables hypoosmotic fish to occupy ice-laden polar waters (DeVries 1971, 1982;  
31 Raymond and DeVries 1977), and allow terrestrial arthropods, such as insects,  
32 spiders, and collembolans, to remain year-round in the cold temperate and polar  
33 areas. The body temperatures of such terrestrial animals may in some cases drop well  
34 below  $-30\text{ }^{\circ}\text{C}$  in winter (Zachariassen and Husby 1982; Duman 2001; Duman et al.  
35 2004; Graham and Davies 2005). Within the animal, AF(G)Ps are known to act by  
36 inactivating structures in the body fluids that could initiate freezing, so-called  
37 ice-nucleating agents (INAs), and by preventing ice from penetrating through the  
38 body wall (Olsen and Duman 1997a, b; Olsen et al. 1998; Duman 2002).

39 AF(G)Ps are categorized as being moderately active or hyperactive, based on the  
40 hysteresis activity they cause at equimolar concentrations. This distinct difference in  
41 antifreeze potency is accompanied by distinct shapes of the ice crystals that form in  
42 their presence; moderately active AF(G)Ps cause bipyramidal crystals to develop, a  
43 shape that only exposes a single crystal plane to the surrounding solution. In the  
44 presence of hyperactive AF(G)Ps, ice crystals express several crystal planes, usually  
45 in the form of hexagonal discs. A number of different factors affect the hysteresis  
46 activity, including their size and the addition of large organic macromolecules and  
47 inorganic ions. This chapter outlines current understanding of the modus operandi of  
48 AF(G)Ps. An attempt is made to provide some simple explanations to the antifreeze  
49 potency of AF(G)Ps, including their characteristics as moderately active or hyper-  
50 active, and how their antifreeze potency is affected by their size and by different  
51 additives. Some characteristics of INAs and their relevance in cold tolerance are also  
52 examined briefly.

## 53 6.2 A Hysteresis Mechanism: The Kelvin Effect

54 The vapor pressure of bulk ice is lower than that of water. Thus, below the melting  
55 point a net transfer of water molecules from the bulk water to ice occurs and the ice  
56 mass grows. However, it follows from the observable fact that ice crystals in the  
57 presence of AF(G)Ps remain unchanged within a temperature interval, that the AF  
58 (G)Ps somehow causes vapor pressure equilibrium between ice and water at all  
59 temperatures within the hysteresis gap. This must be so, since the rate by which  
60 water molecules adds onto the crystal surface must equal the rate by which they  
61 leave. Otherwise, net transfer of water molecules would result, from solution to ice  
62 or vice versa and the crystal would visibly change volume. AF(G)Ps do not lower the  
63 vapor pressure of water any more than other solutes do (Westh et al. 1997). Thus,  
64 they must act by elevating the vapor pressure of the ice to correspond to the higher  
65 vapor pressure of the surrounding solution. The difference between the vapor  
66 pressure of water and ice increases with temperature departure below the equilibrium  
67 melting temperature. Thus, the effect of the AF(G)Ps on the vapor pressure of ice

**Fig. 6.1** Vapor pressure equilibrium within a temperature interval near the melting temperature. For the ice crystal to be stable within the hysteresis gap, the AF(G)Ps must elevate the vapor pressure of the ice surface to correspond to that of the surrounding supercooled solution. This elevation of the vapor pressure must increase with decreasing temperature. Adapted from Kristiansen and Zachariassen (2005)



must be temperature dependent and increase with decreasing temperature, see 68  
Fig. 6.1. 69

Raymond and DeVries (1977) proposed that the AF(G)Ps act by changing the 70  
microscopic growth pattern of the ice surface. Since this is achieved by the AF(G)Ps 71  
becoming irreversibly adsorbed onto the ice surface, they coined the mechanism the 72  
adsorption–inhibition mechanism. Since then, several investigators have had similar 73  
approaches to explaining the phenomenon by irreversible adsorption, including 74  
Wilson (1993) and Kristiansen and Zachariassen (2005). 75

Using fluorescently tagged AFPs, Celik et al. (2013) exchanged the slightly 76  
supercooled solution surrounding an ice crystal. The ice surface of the supercooled 77  
crystals remained fluorescent following the exchange of the surrounding solution, 78  
showing that AFPs were adsorbed onto the crystal surface. Further, the removal of 79  
AFPs in the surrounding solution by the exchange process did not weaken the 80  
hysteresis effect. These observations provide the most unequivocal evidence to 81  
date to show that AF(G)Ps become irreversibly adsorbed onto the ice surface and 82  
that the phenomenon is caused only by the surface-bound AF(G)Ps. Also, Chao et al. 83  
(1995) and DeLuca et al. (1998) found that AF(G)Ps principally operate as mono- 84  
meric units. 85

Elevation of the vapor pressure of the ice by the changed microscopic surface 86  
growth pattern could occur by the so-called Kelvin effect. In the following, a brief 87  
historical outline of the Kelvin effect is provided. This is followed by a description of 88  
how the Kelvin effect is thought to operate at the ice surface. 89

## 90 **6.2.1 The Kelvin Effect: Vapor Pressure at a Curved Interface**

91 In 1871, Prof. William Thomson, later to become first Baron Kelvin, pointed out that  
92 the vapor pressure of water at a concave and a convex surface must be lower and  
93 higher, respectively, than at a plane surface of the water (Thomson 1871). This was  
94 deduced by considering the rise and fall of liquids in a capillary tube as a function of  
95 the curvature of the meniscus; in an atmosphere saturated with vapor, the vapor  
96 pressure decreases with height above the surface of a liquid. Consequently, since a  
97 concave interface in a capillary causes the liquid to come to rest at some fixed height  
98 above the liquid body, Thomson deduced that the vapor pressure at the elevated  
99 concave meniscus is reduced relative to the vapor pressure at the lower plane surface  
100 and must correspond to the lowered saturated atmospheric vapor pressure at that  
101 height. Otherwise, a perpetual net directional motion of water molecules would  
102 develop, as there would be continuous net evaporation at the elevated meniscus  
103 and consequently net condensation at the lower plane surface. Such perpetual motion  
104 of water molecules would violate the fundamental law of thermodynamics. Convex  
105 interfaces must have the opposite effect on the vapor pressure, as such an interface  
106 comes to rest below the plane liquid body where the saturated vapor pressure is  
107 higher. The effect of a surface curvature on the vapor pressure has since become  
108 known as the Kelvin effect.

AU1

### 109 **6.2.1.1 The Critical Radius of Curvature**

110 A decade later, Prof. John Henry Poynting (1881) recognized that the effect of a  
111 surface curvature on the resultant vapor pressure in Thomson's capillary is caused by  
112 a change in the bulk pressure in the water in the capillary; a concave interface evokes  
113 a lower pressure inside the liquid water, as evident from the rise in the capillary, and  
114 hence to a lower vapor pressure, and vice versa for a convex interface. Thus, the  
115 underlying cause of the changing vapor pressure with changing curvature of an  
116 interface is an accompanying curvature-induced change in bulk pressure within the  
117 curved volume.

118 Poynting applied his reasoning to the melting temperature of ice. He inferred that  
119 if the bulk pressure of ice alone was elevated, then the resultant elevated vapor  
120 pressure of the ice would depress the temperature at which the vapor pressures of ice  
121 and water coincides, i.e., a pressure-induced depression of the melting temperature  
122 of the ice surface. By extension, since the pressure-elevating effect of a convexity  
123 increases with decreasing radius, there must be a convexity with a radius small  
124 enough to cause a pressure great enough for ice/water vapor pressure equilibrium to  
125 develop at any temperature below the normal melting point. The radius of this  
126 convexity at a specific temperature is referred to as the critical radius of curvature  
127 at that temperature.

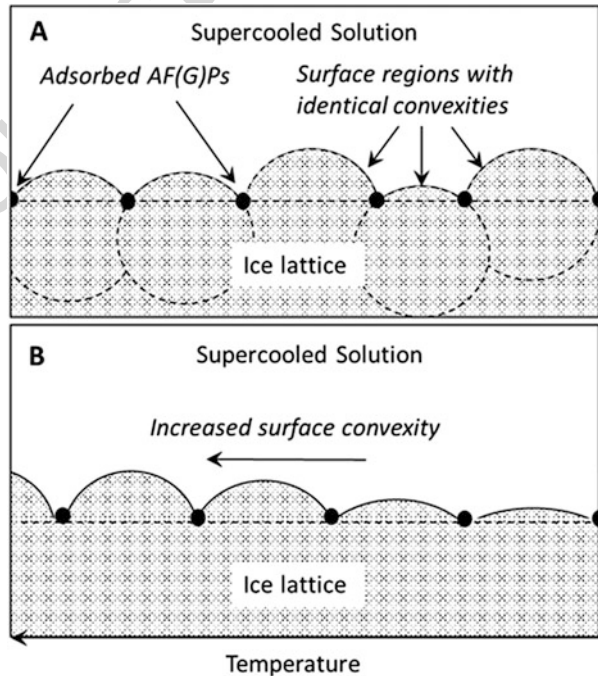
**6.2.2 The Kelvin Effect at the Ice Surface**

It follows from the above paragraphs that AF(G)Ps that are irreversibly adsorbed onto the ice surface could evoke the Kelvin effect by causing the ice surface to grow out as many tiny convex interfaces between them. These convex interfaces would elevate the vapor pressure of the ice surface and, hence, eliminate the difference between the vapor pressures at different temperatures, as illustrated in Fig. 6.1.

The Kelvin effect implies that, at any temperature below the normal melting temperature, the growth of the convex surface zones between the adsorbed AF(G)Ps will halt when they obtain a curvature with a radius corresponding to the critical radius at that temperature. Thus, at any temperature where the phenomenon is expressed, the surface of the entire ice crystal is covered by spherical growth regions with identical convexities, i.e., identical local vapor pressures. This causes the entire ice crystal surface to be in vapor pressure equilibrium with the surrounding supercooled solution, and hence the crystal surface is at its melting temperature, see Fig. 6.2. A. Such a crystal could in principle remain unchanged indefinitely. Crystals in supercooled solutions of AF(G)Ps have been observed for many days without expressing any visible growth (DeVries 1971; Raymond and DeVries 1977; Graether et al. 2000; Fletcher et al. 2001).

As the temperature is lowered further, the many tiny surface zones expand until their convex interfaces again cause vapor pressure equilibrium with the surrounding

**Fig. 6.2** The convexities of the growth zones within the hysteresis gap. (a) All growth zones must have the same convexity at a specific temperature within the hysteresis gap. (b) The convexities increases with decreasing temperature and elevates the vapor pressure of the ice surface in a temperature-dependent manner, as seen in Fig. 6.1. Adapted from Kristiansen and Zachariassen (2005)



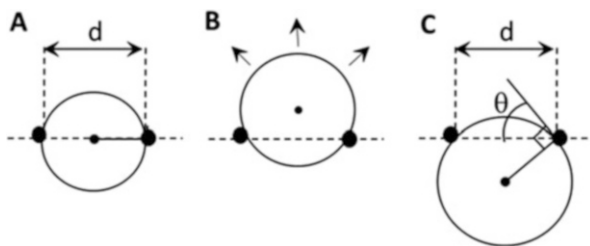


**Fig. 6.3** At the hysteresis freezing point. (a) When one of the convexities has reached the shape of a half-sphere it has reached its maximum convexity. (b) Any further growth of this structure will cause the convexity to decrease and cause spontaneous growth. (c) The relation between adsorbent spacing,  $d$ , and the angle,  $\theta$ . Adapted from Kristiansen and Zachariassen (2005)

148 solution. In this manner ice/water vapor pressure equilibrium is maintained across a  
149 temperature interval, the hysteresis gap, see Figs. 6.1 and 6.2b.

150 There is a limit to how much such a crystal can be cooled, i.e., how convex the  
151 tiny curved interfaces may become; no surface zone can become more convex than  
152 that of a half-sphere. Once such a shape is reached, then any further cooling will  
153 result in the convexity of the structure to decrease on growth. The resultant drop in  
154 vapor pressure due to the reduced convexity will result in spontaneous growth. This  
155 is illustrated in Fig. 6.3a and b. This temperature is the hysteresis freezing point.

### 156 6.3 Hysteresis Activity

157 In the following paragraphs, an attempt is made to explain what fundamentally  
158 determines the hysteresis freezing point, based on the theory outlined above. This  
159 explanation is then extended to incorporate the characteristic difference in activity  
160 between moderately active and hyperactive kinds of AF(G)Ps.

#### 161 6.3.1 *The Largest Intermolecular Adsorbent Gap Determines* 162 *Hysteresis Activity*

163 If only a single one of all the tiny growth zones that protrude out at the crystal surface  
164 should fail, then the hysteresis phenomenon is terminated. Hence, the hysteresis  
165 freezing point is determined by the single growth zone that reaches the shape of a  
166 half-sphere at the highest temperature. Any further growth of this single growth  
167 zone, i.e., any further cooling, will only result in a reduction in its convexity and,  
168 consequently, the phenomenon is terminated.

169 Since all the surface growth zones have the same convexity, it will be the single  
170 one growth zone with the widest diameter that will reach the shape of a half-sphere at

the highest temperature. Thus, the hysteresis freezing point, and therefore the hysteresis activity, is determined by the single largest intermolecular adsorbent spacing between AF(G)Ps that comprise a single growth zone at the crystal surface. Mathematically, the hysteresis activity ( $\Delta T$ ) as a function of the largest such adsorbent spacing,  $d$ , may be expressed as (Kristiansen and Zachariassen 2005):

$$\Delta T = \frac{4\gamma T_E \sin \theta}{\Delta H d}; \quad (6.1)$$

where  $d$  is the spacing in units of cm,  $\gamma$  is the ice/water interfacial tension (taken to be 32 ergs/cm<sup>2</sup>),  $T_E$  is the normal melting temperature for a plane interface (units of K), and  $\Delta H$  is the heat of fusion of water ( $3.3 \cdot 10^9$  ergs/cm<sup>3</sup>).  $\theta$  is an angle describing the situation if a curvature fails before reaching the shape of a half-sphere. For a half-sphere,  $\theta$  is 90° and, hence, the term ( $\sin \theta$ ) is 1. See Fig. 6.3. C for an illustration of the angle  $\theta$ .

### 6.3.2 Moderately Active and Hyperactive AF(G)Ps

There is a great difference in the hysteresis activities caused by different AF(G)Ps. Based on their activities at equimolar concentrations and the shape of the crystals they form in solution, they fall into two categories: hyperactive and moderately active.

Marshall et al. (2004a) found that moderately and hyperactive AFPs accumulate in ice to a similar extent. Also, experimentally determined estimates of average adsorbent spacings between AF(G)Ps on the surface of ice crystals are quite similar in the case of moderately and hyperactive AF(G)Ps; Drori et al. (2015) estimated the average adsorbent distance between hyperactive TmAFP to 7.6–35.2 nm at concentrations ranging from 31.4 to 0.4  $\mu$ M. Comparable results were obtained by Celik et al. (2013) for the same protein. For the moderately active type III AFP, Drori et al. (2015) estimated the average adsorbent distance to be 8.7 to 24.7 nm at concentrations ranging from 19.8 to 1.2  $\mu$ M. Others have estimated similar values for moderately active AF(G)Ps (Wilson et al. 1993; Grandum et al. 1999; Zepeda et al. 2008). Thus, the principal cause of the great difference in the activities of moderately and hyperactive AF(G)Ps do not seem to be due to differences in their preference for ice. Rather, it is likely that the distinct difference between them is the result of the single largest adsorbent gap at the ice surface for some reason is much larger in the case of moderately active AF(G)Ps.



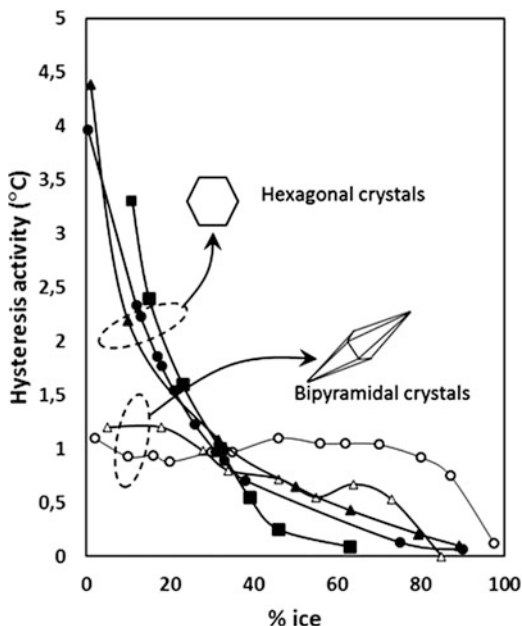
### 202 6.3.2.1 Moderate or Hyperactive: Caused by Plane Specificity 203 and Adsorption Pattern?

204 **Moderate Activity** A characteristic feature of moderately active AF(G)Ps is that  
205 they only adsorb onto a single crystal plane in the ice structure. Notably, none of the  
206 moderately active AF(G)Ps adsorb onto the basal plane of crystals, only onto a single  
207 prism or pyramidal plane (Knight and DeVries 1988; Knight et al. 1991). This plane-  
208 specific adsorption is apparently a consequence of structural features of their  
209 ice-binding sites (IBSs), that restricts these AF(G)Ps to only become irreversibly  
210 adsorbed onto a single plane and orientation. Laursen et al. (1994) showed this by  
211 observing that the moderately active chiral L-AFP I and D-AFP I variants resulted in  
212 adsorption on mirror image directions on the ice surface. The result of such a specific  
213 preference for a single crystal plane is a crystal that only expresses this single  
214 protected crystal plane toward the surrounding supercooled solution. Consequently,  
215 in the presence of moderately active AF(G)Ps crystals obtain a bipyramidal shape, as  
216 this is the only possible crystal shape whose entire surface consists of a single plane.  
217 At the hysteresis freezing point, these bipyramidal crystals freeze out from their  
218 apexes (Raymond and DeVries 1977; Jia and Davies 2002). The fact that they  
219 characteristically grow out of their apexes at the hysteresis freezing point strongly  
220 suggests that the antifreeze potency of moderately active AF(G)Ps are limited by a  
221 large intermolecular spacing at the apex of the bipyramidal crystal (Jia and Davies  
222 2002). This must arise from the fact that these proteins only adsorb onto a single  
223 crystal plane.

224 The surface area involved in determining the hysteresis activity for moderately  
225 active AF(G)Ps is only that miniscule fraction of the total surface area of the crystal  
226 that comprises the two apexes of the bipyramid. Consequently, the hysteresis activity  
227 in the presence of moderately active AF(G)Ps should not be much affected by  
228 changing the total surface area of the ice. Consistent with this, the hysteresis activity  
229 of moderately active AF(G)Ps are reportedly rather insensitive to the amount of ice  
230 present in the sample; large variations in the ice content, i.e., large variations in total  
231 ice crystal surface area, does not appreciably affect the hysteresis activity, see  
232 Fig. 6.4 (Hansen et al. 1991; Wöhrmann 1996; Sørensen and Ramløv 2001).

233 **Hyperactivity** In contrast to the moderately active AF(G)Ps, the hyperactive AF  
234 (G)Ps have been shown to adsorb to several crystal planes that differ greatly in their  
235 orientation, such as both prism and basal planes (Graether et al. 2000; Liou et al.  
236 2000). Structural studies have shown that hyperactive AFPs have IBS that afford the  
237 protein freedom to adsorb in different orientations and on different planes. Their  
238 ability to adsorb onto multiple crystal planes, and most notably the basal plane, is a  
239 feature that separates them from the moderately active AF(G)Ps. Basal plane  
240 adsorption has been implicated as a key feature that causes them to be hyperactive  
241 (Graether et al. 2000; Liou et al. 2000; Pertaya et al. 2008). Because of their ability to  
242 adsorb onto multiple planes, crystals formed in the presence of hyperactive AF(G)Ps  
243 expresses multiple planes to the surrounding supercooled solution and usually take  
244 the form of hexagonal discs (Graether et al. 2000; Liou et al. 2000).

**Fig. 6.4** The dependency of the hysteresis activity on the % ice in the sample. Filled symbols: hyperactive AF(G)Ps. Open symbols: moderately active AFGP. (Filled square) PAGP, a hyperactive AFGP from the nototheniid *Pleuragramma Antarticum* (Wöhrmann 1996). (Filled circle) Hemolymph from *Tenebrio molitor* (Hansen and Baust 1988). (Filled triangle) Hemolymph from *Rhagium inquisitor* (Zachariassen et al. 2002). (Open circle) Serum from *P. antarcticum*. (Open triangle) AFGP from *P. antarcticum* (Wöhrmann 1996). For explanation, see text



Because of their ability to adsorb onto different planes and at different orientations, hyperactive AFPs likely become spread out across the crystal surface in a rather random adsorption pattern. Such a random pattern should, by chance alone, result in the largest adsorption gap increasing with increasing surface area. Consequently, the hysteresis activity of hyperactive AF(G)Ps should decrease with increasing crystal surface area. Consistent with this, several investigators have reported strong dependence of hyperactive AF(G)Ps on the amount of ice present in the sample, see Fig. 6.4 (Zachariassen and Husby 1982; Hansen and Baust 1988; Wöhrmann 1996). As can be seen from the figure, “hyperactivity” is apparently a consequence of using small ice crystals in the experiment, since hyperactive AF(G)Ps have a lower hysteresis activity than their moderately active counterparts at higher contents of ice in the samples.

**The Shape of the Bipyramidal Apexes** When bipyramidal crystals form in the presence of moderately active AF(G)Ps, the ice crystal grows out from the basal planes. Once this bipyramidal shape is formed the crystal stops growing and it remains stable within the hysteresis gap. What is the physical shape of the apex interfaces? Since the moderately active AF(G)Ps do not adsorb onto the basal plane, is the apex a tiny unprotected flat basal plane? If so, then one could envision two-dimensional curved interfaces protruding out only in the direction of the prism planes that form the surrounding edge of the exposed apex basal plane (Raymond and DeVries 1977). The effect of these 2D curvatures that are in the prism plane direction must then also elevate the vapor pressure beyond the base of the curvature toward the center of the flat basal plane in order for vapor pressure

268 equilibrium to persist between the flat apex interface and the surrounding solution.  
269 Another, and perhaps simpler, approach is to assume that the apexes are three-  
270 dimensional spheres protruding out in the basal plane direction. In any event, it is  
271 these areas of the bipyramidal crystal that apparently determines the hysteresis  
272 activity of the moderately active AF(G)Ps.

## 273 **6.4 Factors That Affect the Hysteresis Activity**

274 In the above paragraphs the categorization of AF(G)Ps into moderately active and  
275 hyperactive were ascribed to consequences of irreversible adsorption to the ice  
276 surface that arises from features of their IBS. In the following, differences in  
277 hysteresis activity within each of these categories will be ascribed to the situation  
278 that exist prior to the AF(G)Ps becoming irreversibly adsorbed. It will be argued that,  
279 while the ice crystal is held at the equilibrium melting temperature, AF(G)Ps acquire  
280 an equilibrium distribution between the crystal surface melting region and the  
281 surrounding solution. Then, following a cooling event, AF(G)Ps within this surface  
282 region freeze onto the solidifying crystal surface and, hence, become irreversibly  
283 adsorbed (Kristiansen and Zachariassen 2005). Any change in this distribution  
284 pattern prior to the cooling event will result in changes in the surface density of  
285 irreversibly adsorbed AF(G)Ps after the cooling event and, hence, to changes in the  
286 observed hysteresis activity. Differences in hysteresis activity among hyperactive or  
287 among moderately active AF(G)Ps, may be attributed to differences in the solubility  
288 of the AF(G)Ps in the solution; a lowered solubility results in a shift in the  
289 distribution of the AF(G)Ps toward the ice surface region prior to the cooling  
290 event, and hence, to increased hysteresis activity (Kristiansen and Zachariassen  
291 2005; Kristiansen et al. 2008).

### 292 **6.4.1 The Factors**

293 Several investigators have reported that the size of the AF(G)Ps can have a profound  
294 effect on their capacity to cause thermal hysteresis. For structurally similar isoforms,  
295 their potency reportedly increases with molecular size for both moderately active  
296 AFGPs (Schrage et al. 1982; Chao et al. 1996; Miura et al. 2001; Baardsnes et al.  
297 2003; Nishimiya et al. 2003) and hyperactive AFPs (Leinala et al. 2002; Marshall  
298 et al. 2004b; Liu et al. 2005; Mok et al. 2010; Friis et al. 2014). Synthetic oligomers  
299 of moderately active AFPs also reportedly have increased potency (Nishimiya et al.  
300 2005; Holland et al. 2008; Can and Holland 2011, 2013; Stevens et al. 2015). In all  
301 the cases mentioned above, the increased size is accompanied by an increased IBS or  
302 the addition of multiple IBSs. Other investigators have reported that AFPs are  
303 potentiated by ligation to, or interaction with, large non-ice binding structures  
304 (Deluca et al. 1998; Hakim et al. 2013; Wu and Duman 1991, Wu et al. 1991;

Horwath et al. 1996; Wang and Duman 2005, 2006). In these cases, the IBS is unchanged.

In addition to the effect of molecular size, several authors have reported that the hysteresis activity is also elevated in the presence of various low-mass co-solutes. These low-mass solutes include sugars, polyols, salts, amino acids, salts of polycarboxylates, and NADH. The effect has been reported for both moderately active AF(G)Ps (Kerr et al. 1985; Caple et al. 1986; Evans et al. 2007; Gong et al. 2011) and hyperactive AFPs (Li et al. 1998; Kristiansen et al. 2008; Amornwittawat et al. 2008; Wang et al. 2009a, b; Amornwittawat et al. 2009; Wen et al. 2011; Liu et al. 2015).

There is one thing that variations in molecular size and additives have in common; they change the solubility of proteins in solution. Moreover, they reportedly enhance the hysteresis activity in manners predicted by their general effects on protein solubility. In the following section, the potential importance of the solubility of AF(G)Ps to their antifreeze potency is briefly explored.

#### **6.4.2 The Solubility of the AF(G)Ps: A General Concept to Explain Variability?**

Several authors have in various ways implicated protein solubility as a relevant factor in antifreeze potency (Kristiansen and Zachariassen 2005; Evans et al. 2007; Kristiansen et al. 2008; Wang et al. 2009a). Solubility of AF(G)Ps have also inadvertently been implicated in the manner the AF(G)Ps are thought to orient toward the ice; these proteins are somewhat amphipathic, were the more hydrophobic side that contains the IBS orient toward the ice (Yang et al. 1988; Sönnichsen et al. 1996; Haymet et al. 1998, 1999). In other words, the less soluble side of the molecule orients toward the ice whereas the more soluble side orients toward the water. The logical extension of this is that a less soluble AFP would have a greater affinity toward the ice surface than a more soluble AFP. In the following paragraphs, a brief examination of the significance of this common denominator, the solubility of the AF(G)Ps, to their potency is presented.

##### **6.4.2.1 The AF(G)P/Ice Interaction Is Temperature Dependent**

The ice surface in equilibrium with surrounding liquid water is not distinct but a transition region where the configuration of the water molecules changes from the ordered crystal structure of the ice lattice to the random distribution of the bulk water in the surrounding solution. This change occurs across a 1–2 nm deep region called the interfacial region or the melting/freezing region (Hayward and Haymet 2001).

As stated in the introductory quote by Ramsay (1964), AF(G)Ps act at temperatures below the equilibrium melting temperature of the ice, not at temperatures above

342 it, i.e., the ice crystal does not grow below this temperature but melts above it (but  
343 see also next section concerning superheating of ice crystals). This suggests that the  
344 AF(G)Ps are irreversibly adsorbed onto the ice crystal surface only at temperatures  
345 below the melting temperature. A simple explanation to this is that AF(G)Ps freeze  
346 onto the crystal surface as the temperature is lowered to within the hysteresis gap and  
347 then melt off the ice when the temperature is raised to the melting temperature  
348 (Kristiansen and Zachariassen 2005). Such a temperature-dependent behavior of  
349 freezing onto (adsorption) and melting off (desorption) would explain why ice  
350 crystals in the presence of AF(G)Ps typically melt at the equilibrium temperature  
351 irrespective of any colligative variation in this temperature. It also provides an  
352 intuitive and simple explanation to the long-standing conundrum of the origin of  
353 the necessary bond strength to achieve irreversible adsorption (Wen and Laursen  
354 1992; Knight et al. 1993; Chao et al. 1995); the bond strength between the irrevers-  
355 ibly adsorbed AF(G)P and the ice surface corresponds to those between water  
356 molecules in bulk ice at that temperature. Recently, Garnham et al. (2011a) showed  
357 that the hydration water of a hyperactive AFP has a clathrate-like configuration and  
358 is firmly embedded by extensive H-bonds to the backbone of the protein. Hence, this  
359 crystalline-like water at the IBS appears to be prone to fuse together with the  
360 solidifying crystalline interface once the temperature is lowered and melt off when  
361 the interface disintegrates into chaos on warming to the equilibrium melting tem-  
362 perature. Molecular dynamics studies support this contention (Chakraborty and Jana  
363 2019; Zanetti-Polzi et al. 2019).

364 Pertaya et al. (2008) reported on the fluorescence associated with an ice crystal in  
365 a solution containing fluorescently tagged AFP. When slowly melting a crystal at a  
366 temperature just above that of equilibrium the crystal showed no fluorescence,  
367 indicating no adsorbed AFPs. When cooled to within the hysteresis gap the crystal  
368 surface became fluorescent, indicating irreversible adsorption. Similar results were  
369 reported by Pertaya et al. (2007), who used a technique of photo-bleaching of  
370 fluorescently tagged AFPs to study the AFP/ice association at the crystal surface at  
371 temperatures within, and just above, the hysteresis gap. Bleached AFPs at the surface  
372 were not replaced within the hysteresis gap but were replaced at temperatures just  
373 above, showing that the AFPs were irreversibly adsorbed within the hysteresis gap  
374 and desorbed off the ice at the melting temperature.

375 While in the desorbed state, at the melting temperature of the crystal surface, there  
376 must be a distribution of AF(G)Ps between the melting/freezing region and the bulk  
377 solution. It is this distribution pattern that presumably becomes affected by changes  
378 in the solubility of the AF(G)Ps; a lowered protein solubility means that the AF(G)P  
379 has an increased tendency to move away from the solution and toward the melting/  
380 freezing region. This results in more AF(G)P molecules being at the ice/water  
381 interfacial region and available to freeze onto the solidifying crystal surface the  
382 instant the temperature is lowered. Consequently, lowered solubility of an AF(G)P  
383 should result in greater surface density of the AF(G)P below the melting temperature  
384 and, hence, to greater hysteresis activity (Kristiansen and Zachariassen 2005).

**Superheating of Ice Crystals** Several investigators have reported that ice crystals 385  
in solutions of AF(G)Ps may superheat slightly (Celik et al. 2010; Cziko et al. 2014). 386  
Celik et al. (2010) reported that tiny ice crystals became superheated by 0.04 °C and 387  
0.44 °C in the presence of several hyperactive AFPs. In the case of moderately active 388  
AFP, superheating up to 0.02 °C was reported at high AFP concentrations. The 389  
observed superheating reflects the presence of concave surface regions developing 390  
between irreversibly adsorbed AF(G)Ps at temperatures above the equilibrium 391  
temperature (Knight and DeVries 1989). These observations potentially contradict 392  
the notion of an equilibrium distribution of AF(G)Ps developing between the 393  
solution and the ice surface region at the equilibrium temperature, as outlined above. 394

The samples that expressed this superheating also expressed hysteresis activities 395  
ranging from 1.7 °C to 4.1 °C. The hysteresis activity increases approximately as a 396  
function of the square root of the surface density of AF(G)Ps (Raymond and DeVries 397  
1977; Kristiansen and Zachariassen 2005). Thus, apparently only a small fraction of 398  
the AFPs that was originally frozen onto the surface and caused these high hysteresis 399  
activities was subsequently involved in the comparatively much lower superheating. 400  
That is, most AFPs melted off the ice surface. 401

The superheating phenomenon requires a cooling event to occur; when Celik 402  
et al. (2010) melted out ice in solutions with high concentrations of moderate AFPs 403  
or low concentrations of hyperactive AFPs, they observed that the many small 404  
crystals decreased uniformly in size. If the melting process was briefly halted, then 405  
the crystals began to show slight superheating. This change in melting behavior 406  
following a brief cooling event suggests that AFPs in solution do not adsorb 407  
irreversibly to the ice surface unless there is a cooling event, i.e., the adsorption is 408  
a freezing of the AFPs onto the ice surface. The subsequent desorption as the 409  
temperature is raised is for some of the adsorbed AFPs a delayed process. 410

Why do some of the AF(G)Ps not simply melt off the surface as the temperature is 411  
raised to the melting point? The freezing of the AF(G)Ps onto the ice surface imply 412  
that the hydration water at the IBS becomes part of the crystal lattice. Above its 413  
equilibrium melting temperature, ice melts from its surface, as lattice water mole- 414  
cules are released to the fluid hydrogen-bonding network of the surrounding solu- 415  
tion. However, if no liquid water is in contact with the lattice that is to be melted, 416  
e.g., in the interior of a crystal, the lattice structure may superheat extensively before 417  
a melting nucleation event occurs (Turnbull 1950; Chalmers 1964; Lu and Li 1998). 418  
Consequently, if the crystalline water at the IBS of an adsorbed AFP is shielded from 419  
the surrounding liquid solution, then the melting process at the IBS is prevented and 420  
the AFP will remain adsorbed onto the crystal surface at temperatures above the 421  
melting point. The distinct difference in the capacities of moderately and hyperactive 422  
AFP to cause superheating reported by Celik et al. (2010) presumably reflect 423  
differences in their respective capacities to shield the crystalline water at the IBS 424  
from the surrounding liquid water when adsorbed onto the ice. They observed that in 425  
the presence of hyperactive AFPs, crystals sporadically disappeared over time up to 426  
4 h, showing that this situation can be quite stable if it develops. Since the phenom- 427  
enon is very weak compared to the hysteresis activity, it might be that only those AF 428

429 (G)Ps with certain rare orientations at the crystal surface is able to postpone the  
430 initiation of the melting process at the IBS.

### 431 **6.4.3 Basic Concepts in Solubility Theory**

432 The solubility of a protein in water reflects its energetic state in water (Reynolds et al.  
433 1974). Once present in the water, the solubility of a protein is determined by two  
434 opposing effects acting on structural features of the protein; favorable attractive  
435 forces such as van der Waals- and dipole-type forces lower the energy state of the  
436 protein and therefore increase its solubility. This is opposed by an energetic cost  
437 associated with occupying a cavity within the water that increases its energetic state  
438 and therefore lowers its solubility (Uhlig 1937; Tolls et al. 2002). In the latter case,  
439 the presence of the protein in the water effectively adds additional high-energy water  
440 surface at the water/protein boundary of the cavity occupied by the solute. The  
441 presence of nonpolar surface regions of the protein restricts hydrogen bond forma-  
442 tion between water molecules in the surface boundary, and consequently reduces the  
443 freedom of these local water molecules to orientate. This structuring of water at the  
444 protein/water boundary is known as the hydrophobic effect.

445 According to Uhlig (1937), the solubility ( $S$ ) of a dissolved molecule may be  
446 expressed as:

$$RT \ln(S) = -A\gamma + E \quad (6.2)$$

447 where  $R$  and  $T$  are the universal gas constant and the absolute temperature, respec-  
448 tively. The first term on the right side of Eq. (6.2),  $A\gamma$ , represents the “hydrophobic”  
449 effect that lowers the solubility of a molecule. This effect is a function of the  
450 nonpolar surface area,  $A$ , of the molecule in contact with water, and the energetic  
451 state of the water at this surface, expressed as the water surface tension,  $\gamma$ . This  
452 hydrophobic effect is opposed by the second term on the right-hand side of Eq. (6.2),  
453 the favorable “electrostatic” effect,  $E$ , that raises the solubility of the dissolved  
454 molecule (Reynolds et al. 1974; Melander and Horváth 1977).

455 Changing the size of the AF(G)Ps, for instance by adding or removing repetitive  
456 peptide segments, inadvertently also changes the nonpolar surface area,  $A$ , of the  
457 protein and consequently its solubility. Also, for structurally similar isoforms of  
458 different size, their nonpolar surface areas, and hence, their solubility, correlate with  
459 their size. The small mass solutes that reportedly enhance the hysteresis activity,  
460 such as salts, sugars, polyols, and amino acids are known to elevate the surface  
461 tension,  $\gamma$ , of water (Washburn 1929; Melander and Horváth 1977; Kaushik and  
462 Bhat 1998; Landt 1931; Matubayasi and Nishiyama 2006; Bull and Breese 1974).  
463 Thus, their reported enhancement effect may simply be the result of the solutes  
464 lowering the solubility of the AF(G)P by elevating  $\gamma$  at the protein/water interface.

465 The basic framework outlined above may be useful when interpreting natural and  
466 induced variations in the antifreeze potency among moderately active and among

hyperactive AF(G)Ps. In the following paragraphs, standard solubility theory will be 467  
 applied to examine some of the reported effects small co-solutes and variations in 468  
 size have on hysteresis activity. 469

#### 6.4.4 Low-Mass Additives, Solubility, and Antifreeze Potency 470

The effects of salts on the hysteresis activity in relation to solubility theory will be 471  
 exemplified by the effects of salts on the hyperactive AFP, RiAFP, from the 472  
 cerambycid beetle *Rhagium inquisitor* (Kristiansen et al. 2008). Wang et al. 473  
 (2009a) also had a quite similar approach to this issue. It will be shown that these 474  
 effects are entirely consistent with being caused by salt-induced lowered solubility 475  
 of the RiAFP molecules. To support this claim, the nonpolar surface area and the 476  
 dipole moment of RiAFP is derived from the effects of salts on its antifreeze 477  
 potency. 478

##### 6.4.4.1 The Salting-Out Constant, $K_s$ 479

As mentioned above, salts are known to lower the solubility of proteins. This effect 480  
 is termed “salting-out.” The salting-out effect is qualitatively similar for different 481  
 kinds of proteins and different kinds of salts in that the solubility of the protein 482  
 changes in a log-linear manner with the concentration of salt (Cohn 1925; Melander 483  
 and Horváth 1977): 484

$$\ln(S) = \beta - K_s m \quad (6.3)$$

where  $S$  is the solubility of the protein (mg/ml),  $\beta$  is the solubility of the protein in the 485  
 absence of salts (mg/ml),  $m$  is the concentration of the salt (molal), and  $K_s$  is known 486  
 as the salting-out constant (molal<sup>-1</sup>).  $K_s$  is an expression of the sensitivity of the 487  
 solubility of a particular protein to the presence of a particular salt. The value of  $K_s$  488  
 depends on both the salt and the protein and is experimentally determined as the 489  
 slope of the linear relationship between  $\ln(S)$  and  $m$ . 490

##### 6.4.4.2 Obtaining Salting-Out Constants from Measurements 491 of Hysteresis Activity 492

Since the presence of salts increases the hysteresis activity, adding salts is equivalent 493  
 to increasing the concentration of the AF(G)P. Since solubility is in units of 494  
 concentration, Eq. (6.3) should describe the salt-induced apparent changes in the 495  
 concentration of AF(G)P. Thus, the salting-out constant,  $K_s$ , in the presence of a 496  
 particular salt may be obtained from the hysteresis measurements as follows; the 497  
 actual concentration of AF(G)P in the samples is kept unchanged during the 498



499 procedure. An “apparent” concentration of AF(G)P in the presence of different  
 500 concentrations of salts is then obtained by converting the observed enhanced hys-  
 501 teresis activity in the presence of salts to the equivalent concentration of AF(G)P  
 502 needed to cause this activity in the absence of salt. The value of  $K_s$  for that salt is then  
 503 obtained simply as the slope of the linear relationship obtained by plotting the natural  
 504 logarithm of the “apparent” concentration of AF(G)P in the samples as a function of  
 505 the concentration of salt.

506 Kristiansen et al. (2008) used this method to determine  $K_s$  for each of ten different  
 507 salts from the salt-induced enhancement of the hysteresis activity for RiAFP. As  
 508 predicted by Eq. (6.3) all “apparent” concentrations were log-linear functions of the  
 509 concentrations of the different salts tested.

#### 510 6.4.4.3 The Hofmeister Series and Its Linearity

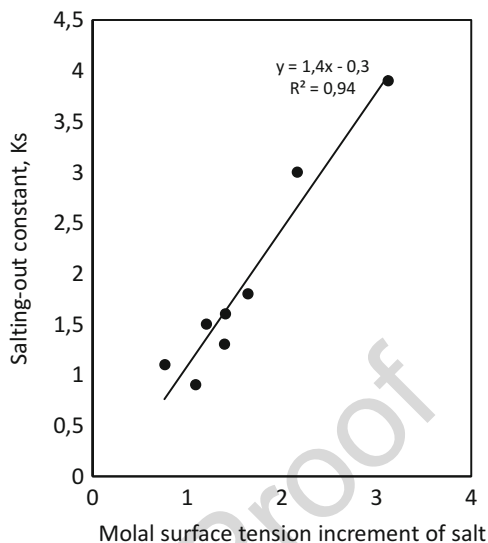
511 An experimentally determined salting-out constant,  $K_s$ , is an expression of the two  
 512 opposing effects acting on structural features of the protein, the favorable “electro-  
 513 static” effect that increases the solubility of the protein and the unfavorable “hydro-  
 514 phobic” effect that lowers its solubility, as outlined in Eq. (6.2). The net observed  
 515 salting-out constant,  $K_s$ , in Eq. (6.3) is given by (Melander and Horváth):

$$K_s = \Omega\sigma - \Lambda \quad (6.4)$$

516 where  $\Omega$  is a protein-specific intrinsic salting-out constant ( $\text{cm dyn}^{-1}$ ),  $\sigma$  is the  
 517 molal surface tension increment of the salt ( $10^{-3} \text{ dyn g/cm mol}$ ), and  $\Lambda$  is a protein-  
 518 specific intrinsic salting-in constant ( $\text{molal}^{-1}$ ).

519 By arranging salts according to their ability to lower the solubility of proteins, the  
 520 so-called Hofmeister series of salts is obtained. The arrangement of different salts in  
 521 the Hofmeister series may be understood from Eq. (6.4); for a specific protein, the  
 522 molal surface tension increment,  $\sigma$ , is the only variable in the equation. Thus, for any  
 523 single protein the arrangement of salts according to their ability to lower the  
 524 solubility of that protein is similar for all proteins and dictated by the molal surface  
 525 tension increment,  $\sigma$ , of the different salts. For example, the following eight salts  
 526 listed in descending order according to their ability to lower protein solubility form  
 527 the Hofmeister series as (value for  $\sigma$  in parenthesis):  $\text{Na}_3\text{C}_6\text{H}_6\text{O}_7$   
 528 (3.12) >  $(\text{NH}_4)_2\text{SO}_4$  (2.16) >  $\text{NaCl}$  (1.64) >  $\text{KCl}$  (1.40) >  $\text{NH}_4\text{Cl}$   
 529 (1.39) >  $\text{NaNO}_3$  (1.20) >  $\text{NaI}$ , (1.09) >  $\text{N}(\text{CH}_3)_4\text{Cl}$  (0.76). Since the value of  $\sigma$  is  
 530 actually the surface tension increment of the water/air interface and not the protein/  
 531 water interface, there are slight differences between the predicted and observed  
 532 Hofmeister series. However, this general arrangement of salts varies little for  
 533 different proteins. Hence, if the salt-induced enhancement of the hysteresis activity  
 534 is caused by salt-induced reduction in the solubility of RiAFP, then the  
 535 enhancement-effect of the different salts should reflect the Hofmeister series. In  
 536 the case of RiAFP the experimentally determined  $K_s$  values were arranged as (value  
 537 for  $\sigma$  in parenthesis):  $\text{Na}_3\text{C}_6\text{H}_6\text{O}_7$  (3.12) >  $(\text{NH}_4)_2\text{SO}_4$  (2.16) >  $\text{NaCl}$  (1.64) >  $\text{KCl}$

**Fig. 6.5** The linearity of the Hofmeister series. Different salting-out constants,  $K_s$ , determined from the hysteresis activity in the presence of different kinds of salts, versus the surface tension increment of the salts used. The slope of the linear line is the intrinsic salting-out constant,  $\Omega$ , for the protein. The intercept value is the intrinsic salting-in constant,  $\Lambda$ , for the protein. These two protein-specific constants may be used to determine the nonpolar surface area and the dipole moment of the protein. Adapted from Kristiansen et al. (2008)



(1.40) >  $\text{NaNO}_3$  (1.20) >  $\text{NH}_4\text{Cl}$  (1.39) >  $\text{N}(\text{CH}_3)_4\text{Cl}$  (0.76) >  $\text{NaI}$  (1.09). This arrangement is in close agreement with the Hofmeister series. An examination of the results of Wang et al. (2009a) also shows that arrangement of the salts according to their ability to enhance a hyperactive AFP, DAFP, from the beetle *Dendroides canadensis* corresponds well with the Hofmeister series. For those salts where the value for  $\sigma$  is known, they are listed as (value for  $\sigma$  in parenthesis);  $\text{NaCl}$  (1.64) >  $\text{KCl}$  (1.40) >  $\text{KBr}$  (1.31) >  $\text{NaBr}$  (1.32) >  $\text{KI}$  (0.84) >  $\text{NaI}$  (1.09) >  $\text{NaClO}_4$  (0.55). In their extensive study, Li et al. (1998) found that, among all the different compounds tested, citrate was the strongest enhancer of the antifreeze potency of DAFP. Citrate has among the highest known surface tension increments ( $\sigma$  of 3.12) and was also the strongest enhancer in the case of RiAFP. Evans et al. (2007) did not find differences in the efficacies of  $\text{LiCl}$ ,  $\text{NaCl}$ , and  $\text{KCl}$  to enhance the antifreeze activity of different kinds of fish AF(G)Ps. This is consistent with the fact that the molal surface tension increments of these salts are very similar, 1.63, 1.64, and 1.40, respectively.

Since both  $\Omega$  and  $\Lambda$  of Eq. (6.4) are constant features of the protein, the  $K_s$  values obtained for that protein will be a linear function of the molal surface tension increment,  $\sigma$ , of the different salts. Figure 6.5 shows that the salting-out constants of RiAFP, determined from the salt-induced enhancement of the hysteresis activity, vary as a linear function of  $\sigma$ , consistent with this prediction of Eq. (6.4). Thus, the linear relationship depicted in Fig. 6.5 is a quantitative representation of the Hofmeister series for RiAFP.

#### 560 6.4.4.4 Quantitative Predictions of Protein Properties from 561 Salt-Induced Enhancement

562 The protein-specific salting-out constant,  $\Omega$ , and the protein-specific salting-in  
563 constant,  $\Lambda$ , of Eq. (6.4) reflect physicochemical properties of the protein (Melander  
564 and Horváth 1977). Thus, if the concept of solubility-induced enhancement is  
565 correct, then it should be possible to use the information derived from the antifreeze  
566 measurements to predict features of the protein that are reflected by these constants.

567 The protein-specific salting-out constant,  $\Omega$ , of Eq. (6.4) represents the hydro-  
568 phobic properties of the protein and is a function of its nonpolar surface area,  $\phi$ . The  
569 numeric value of  $\phi$ , in units of square Ångström, may be obtained from  $\Omega$  as  
570 (Melander and Horváth 1977):

$$\phi = 411\Omega - 12 \quad (6.5)$$

571 According to Eq. (6.4),  $\Omega$  is given by the slope of the linear relationship depicted  
572 in Fig. 6.5. Using the value of  $1.4 \text{ cm dyn}^{-1}$  for  $\Omega$  in Eq. (6.5) gives a value for  $\phi$  for  
573 RiAFP of  $563 \text{ \AA}^2$ . This is about 20% of the total surface area of the protein  
574 (Kristiansen et al. 2008). According to Melander and Horváth (1977),  $\phi$  is typically  
575 between 20% and 40% of the total surface area of proteins. The sensitivity of RiAFP  
576 to become enhanced by salts therefore seems to correspond well with the expected  
577 salt sensitivity of a protein of its size.

578 The intrinsic protein salting-in constant,  $\Lambda$ , of Eq. (6.4) reflects the favorable  
579 electrostatic forces acting to enhance the solubility of the protein and is a function of  
580 its dipole moment,  $\mu$ . The dipole moment,  $\mu$ , may be numerically obtained in units of  
581 Debye from  $\Lambda$  using the formula (Melander and Horváth 1977):

$$\mu = -578\Lambda \quad (6.6)$$

582 According to Eq. (6.4), the value of  $\Lambda$  is given by the intercept of the linear  
583 relationship depicted in Fig. 6.5 and has the value of  $-0.3 \text{ molal}^{-1}$ . This gives a  
584 predicted dipole moment for RiAFP of 173 Debye. Since the original study was  
585 published (Kristiansen et al. 2008), the crystal structure of RiAFP has become  
586 available (Hakim et al. 2013). The structure file (PDB 4DT5) contains two mole-  
587 cules, A and B, which, when submitted to the online Protein Dipole Moments Server  
588 (Felder et al. 2007) has predicted dipole moments of 182 Debye and 125 Debye,  
589 respectively. It is noteworthy that the dipole moment of RiAFP, derived from its  
590 molecular structure, coincides within a few percentage points with the dipole  
591 moment derived from the effects of salts on the antifreeze potency of the protein.

592 Considering the above presented relations, it appears obvious that salts enhance  
593 the antifreeze potency by lowering the solubility of AF(G)Ps. Since the other small  
594 mass solutes known to enhance the antifreeze potency of AF(G)P, i.e., polyols,  
595 amino acids, sugars etc., act on protein solubility in a manner similar to that of salts,  
596 they are all likely to operate by the same mechanism.

### 6.4.5 Molecular Size, Solubility, and Antifreeze Potency

597

Several explanations are provided for the effect of size on the potency of AF(G)Ps. In those cases where the IBS does not vary with the size of the protein, the size effect is ascribed to the larger AFP–macromolecule complex covering a larger surface area than the AFP alone. This larger coverage effectively reduces the intermolecular adsorbent gap between adsorbed AFPs at the ice surface, thereby displacing the hysteresis freezing point to a lower temperature (Wu et al. 1991). When the variation in molecular size of the protein involves changes in the size of the IBS, then the effect has additionally been ascribed to various aspects of their ice-binding ability (Leinala et al. 2002; Mok et al. 2010; Chao et al. 1996; Liu et al. 2005). The increased potency reported for a natural and several synthetic intramolecular multimers of AFPs is ascribed to an overall greater likelihood of successful adsorption due to the presence of multiple IBSs (Miura et al. 2001; Nishimiya et al. 2003) or to increased overall ice-binding area (Baardsnes et al. 2003).

Although some, or even all, of these explanations may contribute to some extent to the observed effect, there are nevertheless problems associated with their applicability. For instance, Marshall et al. (2004b) pointed out that, explanations relying on differences in interaction energies at the IBS are not likely to be correct, since AF(G)Ps are irreversibly adsorbed onto the ice surface, i.e., it is an all-or-none situation. As alluded to above (Sect. 6.4.2), if the AF(G)Ps become irreversibly adsorbed by freezing onto the interface, then they are as strongly adsorbed to the ice as any piece of ice is to the surface of ice. Thus, changing the size of the IBS, or the like, should not make any difference. In the case of the added surface cover explanation provided by Wu et al. (1991), it is intuitively logical and could well be a satisfactory explanation. However, as pointed out by the original authors, experimentally there is no correlation between the size of the enhancer and the enhancement effect (Wu and Duman 1991). The enhancers, identified by Wu and Duman (1991), range according to efficiency as 70 kDa (endogen enhancer) > 70 kDa (protein ice nucleator) > 800 kDa (lipoprotein ice nucleator) > 150 kDa (antibody) > gelatin (80–375 kDa) > agar (average 120 kDa). The effectiveness of all these enhancers is surpassed by a 28 kDa endogenous enhancer (Wang and Duman 2006). Also, Horwath et al. (1996) reported that an efficient endogenous enhancer from the beetle *Tenebrio molitor* was 12 kDa, about the same size as the AFP. Thus, there seem to be little experimental support for the otherwise logical contention that the enhancement effect of size arises from added surface cover of the adsorbent complex.

Equation (6.2) provides a general explanation to the size effect; variations in size is inevitably accompanied by variations in the nonpolar surface area,  $A$ , of the protein and probably also variations in the electrostatic forces,  $E$ , acting between the protein and the solution. Such size-induced differences in solubility is consistent with the gradual increase in antifreeze potency with size that are reported for structurally similar variants of both hyperactive and moderately active AF(G)Ps. This approach also provides an explanation as to why there is no correlation between antifreeze potency and size for macromolecules that are very different; if the

640 structures are different, then differences in their nonpolar surface areas and the  
641 strength of the electrostatic forces acting between the structure and the surrounding  
642 water do not vary with size. In other words, the solubility of structurally different  
643 compounds does not vary with molecular size. This would explain why a 28 kDa  
644 protein is a far more efficient enhancer than a protein of 800 kDa; the smaller is  
645 simply less soluble.

646 Some complicated and intriguing findings have been reported that ties in well  
647 with the concept of solubility-induced enhancement; Wang and Duman (2005)  
648 found that certain of the isoforms of hyperactive AFPs, DAFPs, from  
649 *D. canadensis* interact, and the association results in greater activities. This greater  
650 activity may be ascribed to a reduced solubility due to the overall larger nonpolar  
651 surface area,  $\phi$ , of the complex (Eqs. 6.2, 6.4 and 6.5). But further, they found that  
652 the additive glycerol only acted as an enhancer if the isoforms interacted. This may  
653 also be understood from Eqs. (6.4) and (6.5); the sensitivity of a protein to some  
654 additive increases with increased nonpolar surface area,  $\phi$ . It should be noted that  
655 several of the polyols, glycerol included, actually reduces the surface tension of  
656 water. Nevertheless, Gekko and Timasheff (1981) found that glycerol lowered the  
657 solubility of proteins by the same mechanism as salts, i.e., polyols act differently at  
658 the air/water interface than at the protein/water interface.

659 Amornwittawat et al. (2008) found that many carboxylates enhanced DAFPs and  
660 ascribed the effect to aggregation of DAFPs. As in the case with Wang and Duman  
661 (2005), such aggregation results in lowered solubility due to increased overall  
662 nonpolar surface area, which could explain the increased activity. Wang et al.  
663 (2009b) identified the binding sites for these carboxylates to be specific arginine  
664 residues in the DAFP structure, since blocking these residues abolished the effect.  
665 With intact such residues the monomeric DAFP aggregated in the presence of  
666 carboxylates and the complex was more sensitive to other additives. This situation  
667 is similar to that of Wang and Duman (2005) described above, i.e., the greater  
668 nonpolar surface area,  $\phi$ , of the complex makes the overall complex more sensitive  
669 to additives than the monomers alone (Eqs. 6.2, 6.4 and 6.5).

670 As have been outlined above, ascribing variations in antifreeze potency to  
671 variations in protein solubility explain many aspects of hysteresis activity, including  
672 the significance of size and how additives enhance AF(G)Ps. This approach also  
673 explains why interactions between isoforms cause enhancement and the increased  
674 sensitivity to additives when isoforms interact. Ascribing variability of antifreeze  
675 potency to variations in protein solubility give a plausible explanation to the natural  
676 variability reported among AF(G)Ps that are either hyperactive or moderately active.  
677 Both qualitative and quantitative agreements with predictions based on established  
678 theory support this approach.

679 The presence of a 1 molal solution of sodium citrate has the effect on the  
680 hysteresis activity of RiAFP equivalent to elevating its concentration 50-fold  
681 (Kristiansen et al. 2008). Thus, aside from the categorization into hyperactive and  
682 moderately active, which are consequences of structural aspects of their IBS, the  
683 physicochemical property of solubility is probably the most dominant determinant of  
684 AF(G)P potency.

## 6.5 AF(G)Ps and Ice Nucleation

685

The convex surface zones that grow out at the ice surface within the hysteresis gap 686 are developing ice nuclei with their critical radius at that temperature. At the 687 hysteresis freezing point, the phenomenon is terminated by a surface nucleation 688 event, as one of these surface nuclei initiates nucleation. Apart from causing thermal 689 hysteresis by controlling the development of nuclei at the ice surface, AFPs also 690 interact with structures in the body fluids that can trigger an ice nucleation event. 691 Such a structure is known as an ice-nucleating agent, INA, and the nucleation 692 process triggered by INAs is referred to as heterogeneous nucleation. This is to 693 distinguish this kind of nucleation from that which occur by spontaneous ordering of 694 water, so-called homogenous nucleation. Evidence suggest that the ice nucleation 695 sites of INAs are structurally related to the IBSs of AFPs. Thus, the mechanism of ice 696 nucleation by INAs may be very similar to the mechanism of adsorption of AFPs 697 to ice. 698

### 6.5.1 Biological Relevance of INAs

699

Freeze-avoiding species die if their body fluids freeze out. Consequently, they rely 700 on extensive supercooling of their body fluids to survive subfreezing temperatures. 701 Any incidental INAs in the body fluids of such an organism would therefore be 702 potentially lethal. Freeze-avoiding insects are known to remove or reduce the 703 amount of such incidental INAs that could pose a threat (Neven et al. 1986; Olsen 704 and Duman 1997a, b). In addition, AFPs prevent incidental INAs from initiating 705 freezing by physically interacting with such structures (Olsen and Duman 1997a, b; 706 Duman 2002). By removal of INAs from their body fluids and by producing high 707 concentrations of AFPs, the supercooling points of freeze avoiding larvae of the 708 pychroid beetle *Dendroides canadensis* changes from about  $-7^{\circ}\text{C}$  in the summer to 709 below  $-30^{\circ}\text{C}$  during winter (Olsen and Duman 1997a, b). 710

Freeze-tolerant species, that adaptively allow their body fluids to freeze out, often 711 produce INAs and allocate them to the extracellular fluid. The principal function of 712 such adaptive INAs in freeze tolerance is to prevent harmful cellular freezing by 713 initiating a preemptive nucleation event outside the cells at a temperature above the 714 nucleation temperature of any incidental harmful cellular INAs (Zachariassen and 715 Hammel 1976). Since solutes are excluded from the growing ice mass, the extracel- 716 lular freezing event causes the remaining unfrozen extracellular fluid fraction to 717 become increasingly concentrated. This in turn initiates a concomitant osmotic 718 efflux of water out from the cells. The extracellular freezing process and consequent 719 efflux of cell water continues until the melting point of the remaining unfrozen fluid 720 fraction is colligatively depressed to the environmental temperature, at which point 721 the danger of harmful cellular freezing is eliminated. 722

723 **6.5.2 Overall Structural Aspects of INAs**

724 It is vital for the functionality of adaptive INAs found in freeze-tolerant species that  
725 their nucleation temperature is above that of any incidental harmful cellular INAs.  
726 The efficiency of INAs to initiate nucleation depends on their size. This may be  
727 understood from Eq. (6.1); the larger the diameter of the INA,  $d$ , the less  
728 supercooling,  $\Delta T$ , is required to initiate nucleation. Consistent with this, adaptive  
729 INAs found in freeze tolerant species are very large structures. It is likely that the  
730 great potency of biologically adaptive INAs results from association between  
731 monomeric INA molecules; it has been shown that an adaptive 800 kDa INA from  
732 freeze-tolerant larvae of the crane fly, *Tipula trivittata*, form long chains of 800 kDa  
733 monomers, akin to pearls-on-a-string, and that two such chains align side by side  
734 into extended dimers (Yeung et al. 1991). This association apparently relies on the  
735 presence of phosphatidylinositol, PI, at the surface of the INA, as enzymatic removal  
736 of PI depressed the nucleation temperature (Neven et al. 1989). PI has also been  
737 shown to anchor highly active bacterial INAs to the bacterial membrane (Kozloff  
738 et al. 1991) and thereby possibly causing them to cooperate. The proposed structure  
739 of a large repetitive segment of the 123 kDa INA from *Pseudomonas borealis*  
740 suggests that the operating INA consists of at least two monomers (Garnham et al.  
741 2011b).

742 AFPs are known to physically interact with INA molecules (Wu and Duman  
743 1991). A simple explanation to how AFPs depress the nucleation temperature of  
744 INAs would be if they act by preventing them from forming larger associations,  
745 analogous to the effect of reducing the diameter of growing surface nuclei at the ice  
746 surface (Eq. 6.1). A peculiar aspect of this AFP/INA association is that it apparently  
747 does not involve the IBS of the AFP (Duman 2001). This is evident from the fact that  
748 the hysteresis activity, which requires the IBS to be free to adsorb onto the ice  
749 surface, is enhanced by the AFP/INA interaction (Wu and Duman 1991). It remains  
750 unclear if AFPs contain some secondary functional surface-site outside the IBS  
751 dedicated to the interaction of structures other than ice (Duman 2001).

752 Although the details of how INAs trigger freezing is not entirely identified, it is  
753 likely that they do so by structuring their hydration water to mimic that of ice. It has  
754 been shown that the hydration water at the IBS of  $\beta$ -helical hyperactive AFPs are  
755 clathrate-like, and this structured water has been implicated in the process of  
756 adsorption (Garnham et al. 2011a). Large internal repetitive parts of several bacterial  
757 INAs have been modeled to fold into  $\beta$ -helices (Graether and Jia 2001; Garnham  
758 et al. 2011b). The structural similarity between the IBS of the  $\beta$ -helical AFPs and the  
759 suspected nucleation sites of the INAs suggest they share a similar mode of opera-  
760 tion. Supporting this contention, Kobashigawa et al. (2005) reported that a recom-  
761 binant protein corresponding to an internal part of one of these bacterial INAs shape  
762 ice crystals into hexagonal bipyramids. Similar results were also reported by Xu  
763 et al. (1998), who found that a 164 kDa molecule with INA activity shaped ice  
764 crystals into hexagonal bipyramids. Apparently, these bacterial INAs have some  
765 kind of internal IBS. It is not clear if the part of the INA responsible for the observed

structuring of the ice, an IBS, corresponds to the site that causes nucleation. Another 766  
aspect is the shape of the ice crystals in the presence of the INAs reported by 767  
Kobashigawa et al. (2005); these INAs are those of the species *Pseudomonas* 768  
*syringae*, the same INA modeled as a  $\beta$ -helix by Graether and Jia (2001). The ice 769  
crystals in the presence of all known  $\beta$ -helical AFPs express multiple ice crystal 770  
planes, e.g., in the form of hexagonal discs. These INAs, on the other hand, shape ice 771  
into hexagonal bipyramids, as seen in the presence of the monoplane-specific AF(G) 772  
Ps of fish. 773

If the IBS of AF(G)Ps is structurally comparable to the nucleation sites of INAs, 774  
then why are AF(G)Ps not INAs? The explanation may in part rely on differences in 775  
the structure of the hydration water at the IBS/nucleation site and in part be due to the 776  
large difference in size of AFPs and INAs. What is clear is that  $\beta$ -helical insect AFPs 777  
do not act as INAs within the supercooling range of the freeze avoiding insects, i.e., 778  
down to about  $-30\text{ }^{\circ}\text{C}$ , or even below. 779

## 6.6 Conclusions 780

This chapter has dealt with the modus operandi of AF(G)Ps. The characteristic 781  
prevention of ice growth within the hysteresis gap is explained by ice/water vapor 782  
pressure equilibrium being maintained by the Kelvin effect as the ice surface grows 783  
out as microscopic curvatures between adsorbed AF(G)Ps. The different potencies 784  
of moderately and hyperactive AF(G)Ps are ascribed to differences in their adsorp- 785  
tion habits, whereas variations in antifreeze potencies within each of these categories 786  
are ascribed to variations in their solubilities. In the latter case, experimental proof of 787  
concept is discussed in the context of basic solubility theory. Some characteristics of 788  
ice-nucleating agents (INAs) in relation to AF(G)Ps and their relevance in cold 789  
tolerance was also briefly examined. 790

AF(G)Ps as a group are defined by their shared capacity to prevent ice in solution 791  
from growing at temperatures below the melting point. However, another wide- 792  
spread trait observed for many of these proteins when at very low concentrations 793  
occurs at the melting temperature; they inhibit the spontaneous process by which 794  
larger ice crystals grow at the expense of smaller crystals. This trait is not an 795  
exclusive property of AF(G)Ps but are also found among non-antifreeze proteins 796  
and organic solutes. This fascinating phenomenon of recrystallisation inhibition is 797  
both biologically and commercially important and is the topic of the next chapter. 798

## References 799

- Amornwittawat N, Wang S, Duman JG, Wen X (2008) Polycarboxylates enhance beetle antifreeze 800  
protein activity. *Biochim Biophys Acta* 1784:1942–1948 801



- 802 Amornwittawat N, Wang S, Banatlo J, Chung M, Velasco E, Duman JG, Wen X (2009) Effects of  
803 polyhydroxy compounds on beetle antifreeze protein activity. *Biochim Biophys Acta*  
804 1794:341–346
- 805 Baardsnes J, Kuiper MJ, Davies PL (2003) Antifreeze protein dimer. When two ice binding faces  
806 are better than one. *J Biol Chem* 278:38942–38947
- 807 Bull HB, Breese K (1974) Surface tension of amino acid solutions: a hydrophobicity scale of amino  
808 acid residues. *Arch Biochem Biophys* 161:665–670
- 809 Can O, Holland NB (2011) Conjugation of type I antifreeze protein to polyallylamine increases  
810 thermal hysteresis activity. *Bioconjug Chem* 22:2166–2171
- 811 Can O, Holland NB (2013) Utilizing avidity to improve antifreeze protein activity: a type III  
812 antifreeze protein trimer exhibits increased thermal hysteresis activity. *Biochemistry*  
813 52:8745–8752
- 814 Caple G, Kerr WL, Burcham TS, Osuga DT, Yeh Y, Feeney RE (1986) Superadditive effects in  
815 mixtures of fish antifreeze glycoproteins and polyalcohols or surfactants. *J Colloid Interface Sci*  
816 111:299–304
- 817 Celik Y, Graham LA, Mok Y-F, Bar M, Davies PL, Braslavsky I (2010) Superheating of ice crystals  
818 in antifreeze protein solutions. *Proc Natl Acad Sci* 107:5423–5428
- 819 Celik Y, Drori R, Pertaya-Braun N, Altan A, Barton T, Bar-Dolev M, Groisman A, Davies PL,  
820 Braslavsky I (2013) Microfluidic experiments reveal that antifreeze proteins bound to ice  
821 crystals suffice to prevent their growth. *Proc Natl Acad Sci* 110:1309–1314
- 822 Chakraborty S, Jana B (2019) Ordered hydration layer mediated ice adsorption of a globular  
823 antifreeze protein: mechanistic insight. *Phys Chem Chem Phys* 21:19298–19310
- 824 Chalmers B (1964) Principles of solidification. Wiley, New York
- 825 Chao H, DeLuca CL, Davies PL (1995) Mixing antifreeze protein types changes ice crystal  
826 morphology without affecting antifreeze activity. *FEBS Lett* 357:183–186
- 827 Chao H, Hodges RS, Kay CM, Gauthier SY, Davies PL (1996) A natural variant of Type I  
828 antifreeze protein with four ice-binding repeats is a particularly potent antifreeze. *Protein Sci*  
829 5:1150–1155
- 830 Cohn EJ (1925) The physical chemistry of the proteins. *Physiol Rev* 5:349–437
- 831 Cziko PA, DeVries AL, Evans CW, Cheng C-HC (2014) Antifreeze protein-induced superheating  
832 of ice inside Antarctic notothenioid fishes inhibits melting during summer warming. *Proc Natl*  
833 *Acad Sci* 111:14583–14588
- 834 DeLuca CI, Comley R, Davies PL (1998) Antifreeze proteins bind independently to ice. *Biophys J*  
835 74:1502–1508
- 836 DeVries AL (1971) Glycoproteins as biological antifreeze agents in Antarctic fishes. *Science*  
837 172:1152–1155
- 838 DeVries AL (1982) Biological antifreeze agents in Coldwater fishes. *Comp Biochem Physiol A*  
839 73:627–640
- 840 Drori R, Davies PL, Braslavsky I (2015) Experimental correlation between thermal hysteresis  
841 activity and the distance between antifreeze proteins on an ice surface. *RSC Adv* 5:7848–7853
- 842 Duman JG (2001) Antifreeze and ice nucleator proteins in terrestrial arthropods. *Annu Rev Physiol*  
843 63:327–357
- 844 Duman JG (2002) The inhibition of ice nucleators by insect antifreeze proteins is enhanced by  
845 glycerol and citrate. *J Comp Physiol B* 172:163–168
- 846 Duman JG, Bennett V, Sformo T, Hochstrasser R, Barnes BM (2004) Antifreeze proteins in  
847 Alaskan insects and spiders. *J Insect Physiol* 50:259–266
- 848 Evans PE, Hobbs RS, Goddard SV, Fletcher GL (2007) The importance of dissolved salts to the  
849 *in vivo* efficacy of antifreeze proteins. *Comp Biochem Physiol A* 148:556–561
- 850 Felder CE, Prilusky J, Silman I, Sussman JL (2007) A server and database for dipole moments of  
851 proteins. *Nucleic Acids Res* 35:W512–W521. <http://dipole.weizmann.ac.il/>
- 852 Fletcher GL, Hew CL, Davies PL (2001) Antifreeze proteins in teleost fishes. *Annu Rev Physiol*  
853 63:359–390

- Friis DS, Kristiansen E, von Solms N, Ramløv H (2014) Antifreeze activity enhancement by site directed mutagenesis on an antifreeze protein from the beetle *Rhagium mordax*. FEBS Lett 588:1767–1772 854–856
- Garnham CP, Campbell RL, Davies PL (2011a) Anchored clathrate waters bind antifreeze proteins to ice. Proc Natl Acad Sci 108:7363–7367 857–858
- Garnham CP, Campbell RL, Walker VK, Davies PL (2011b) Novel dimeric  $\beta$ -helical model of an ice nucleation protein with bridged active sites. BMC Struct Biol 11:36 859–860
- Gekko K, Timasheff SN (1981) Mechanism of protein stabilization by glycerol: preferential hydration in glycerol-water mixtures. Biochemistry 20:4667–4676 861–862
- Gong HS, Croft K, Driedzic WR, Ewart VK (2011) Chemical chaperoning action of glycerol on the antifreeze protein of rainbow smelt. J Therm Biol 36:78–83 863–864
- Graether SP, Jia Z (2001) Modeling *Pseudomonas syringae* ice-nucleation protein as a  $\beta$ -helical protein. Biophys J 80:1169–1173 865–866
- Graether SP, Kuiper MJ, Gagné SM, Walker VK, Jia Z, Sykes BD, Davies PL (2000)  $\beta$ -helix structure and ice-binding properties of a hyperactive antifreeze protein from an insect. Nature 406:325–328 867–869
- Graham LA, Davies PL (2005) Glycine-rich antifreeze proteins from snow fleas. Science 310:461 870
- Grandum S, Yabe A, Nakagomi K, Tanaka M, Takemura F, Kobayashi Y, Frivik P-E (1999) Analysis of ice crystal growth for a crystal surface containing adsorbed antifreeze proteins. J Cryst Growth 205:382–390 871–873
- Hakim A, Nguyen JB, Basu K, Zhu DF, Thakral D, Davies PL, Isaacs FJ, Modis Y, Meng W (2013) Crystal structure of an insect antifreeze protein and its implications for ice binding. J Biol Chem 288:12295–12304 874–876
- Hansen TN, Baust JG (1988) Serial dilution of *Tenebrio molitor* haemolymph: analysis of antifreeze activity by differential scanning calorimetry. Cryo-Letters 9:386–391 877–878
- Hansen TN, DeVries AL, Baust JG (1991) Calorimetric analysis of antifreeze glycoproteins of the polar fish, *Dissostichus mawsoni*. Biochim Biophys Acta 1079:169–173 879–880
- Haymet ADJ, Ward LG, Harding MM, Knight CA (1998) Valine substituted winter flounder ‘antifreeze’: preservation of ice growth hysteresis. FEBS Lett 430:301–306 881–882
- Haymet ADJ, Ward LG, Harding MM (1999) Winter flounder ‘antifreeze’ proteins: synthesis and ice growth inhibition of analogues that probe the relative importance of hydrophobic and hydrogen-bonding interactions. J Am Chem Soc 121:941–948 883–885
- Hayward JA, Haymet ADJ (2001) The ice/water interface: molecular dynamics simulations of the basal, prism, 2021 and 2110 interfaces of ice Ih. J Chem Phys 114:3713–3726 886–887
- Holland NB, Nishimiya Y, Tsuda S, Sönnichsen FD (2008) Two domains of RD3 antifreeze protein diffuse independently. Biochemistry 47:3955–3941 888–889
- Horwath KL, Easton CM, Poggioli GJ Jr, Myers K, Schnorr IL (1996) Tracking the profile of a specific antifreeze protein and its contribution to the thermal hysteresis activity in cold hardy insects. Eur J Entomol 93:419–433 890–891
- Jia Z, Davies PL (2002) Antifreeze proteins: an unusual receptor-ligand interaction. Trends Biochem Sci 27:101–106 892–894
- Kaushik JK, Bhat R (1998) Thermal stability of proteins in aqueous polyol solutions: role of the surface tension of water in the stabilizing effect of polyols. J Phys Chem B 102:7058–7066 895–896
- Kerr WL, Burcham TS, Osuga DT, Yeh Y, Feeney RE (1985) Synergistic depression of the freezing temperature in solutions of polyhydroxy compounds and antifreeze glycoproteins. Cryo-Letters 6:107–114 897–899
- Knight CA, DeVries AL (1988) The prevention of ice crystal growth from water by ‘antifreeze proteins’. In: Wagner PE, Vali G (eds) Atmospheric aerosols and nucleation. Lecture notes in physics 309. Springer, Berlin 900–902
- Knight CA, DeVries AL (1989) Melting inhibition and superheating of ice by an antifreeze glycopeptide. Science 245:505–507 903–904
- Knight CA, Cheng CC, DeVries AL (1991) Adsorption of  $\alpha$ -helical antifreeze peptides on specific ice crystal surface planes. Biophys J 59:409–418 905–906

- 907 Knight CA, Driggers E, DeVries AL (1993) Adsorption to ice of fish antifreeze glycopeptides 7 and  
908 8. *Biophys J* 64:252–259
- 909 Kobashigawa Y, Nishimiya Y, Miura K, Ohgiya S, Miura A, Tsuda S (2005) A part of ice  
910 nucleation protein exhibits the ice-binding ability. *FEBS Lett* 579:1493–1497
- 911 Kozloff LM, Turner MA, Arellano F, Lute M (1991) Phosphatidylinositol, a phospholipid of  
912 ice-nucleating bacteria. *J Bacteriol* 173:2053–2060
- 913 Kristiansen E, Zachariassen KE (2005) The mechanism by which fish antifreeze proteins cause  
914 thermal hysteresis. *Cryobiology* 51:262–280
- 915 Kristiansen E, Pedersen SA, Zachariassen KE (2008) Salt-induced enhancement of antifreeze  
916 protein activity: a salting-out effect. *Cryobiology* 57:122–129
- 917 Landt E (1931) The surface tension of solutions of various sugars. *Z Ver Dtsch Zucher-Ind*  
918 81:119–124
- 919 Laursen RA, Wen D, Knight CA (1994) Enantioselective adsorption of the D- and L-forms of an  
920  $\alpha$ -helical antifreeze polypeptide to the {2021} planes of ice. *J Am Chem Soc* 116:12057–12058
- 921 Leinala EK, Davies PL, Doucet D, Tyshenko MG, Walker VK, Jia Z (2002)  $\beta$ -Helical antifreeze  
922 protein isoform with increased activity. *J Biol Chem* 277:33349–33352
- 923 Li N, Andorfer C, Duman JG (1998) Enhancement of insect antifreeze protein activity by solutes of  
924 low molecular mass. *J Exp Biol* 201:2243–2251
- 925 Liou YC, Tocilj A, Davies PL, Jia Z (2000) Mimicry of ice structure by surface hydroxyls and water  
926 of a beta-helix antifreeze protein. *Nature* 406:322–324
- 927 Liu K, Jia Z, Chen G, Tung C, Liu R (2005) Systematic size study of an insect antifreeze protein and  
928 its interaction with ice. *Biophys J* 88:953–958
- 929 Liu Z, Li H, Pang H, Me J, Mao X (2015) Enhancement effect of solutes of low molecular mass on  
930 the insect antifreeze protein ApAFP752 from *Anatolica polita*. *J Therm Anal Calorim*  
931 120:307–315
- 932 Lu K, Li Y (1998) Homogeneous nucleation catastrophe as a kinetic stability limit for superheated  
933 crystal. *Phys Rev Lett* 80:4474–4477
- 934 Marshall CB, Tomczak MM, Gauthier SY, Kuiper MJ, Lankin C, Walker VK, Davies PL (2004a)  
935 Partitioning of fish and insect antifreeze proteins into ice suggests they bind with comparable  
936 affinity. *Biochemistry* 43:148–154
- 937 Marshall CB, Daley ME, Sykes BD, Davies PL (2004b) Enhancing the activity of a  $\beta$ -helical  
938 antifreeze protein by the engineered addition of coils. *Biochemistry* 43:11637–11646
- 939 Matubayasi N, Nishiyama A (2006) Thermodynamic quantities of surface formation of aqueous  
940 electrolyte solutions VI. Comparison with typical nonelectrolytes, sucrose and glucose. *J*  
941 *Colloid Interface Sci* 298:910–913
- 942 Melander W, Horváth C (1977) Salt effects on hydrophobic interactions in precipitation and  
943 chromatography of proteins: an interpretation of the lyotropic series. *Arch Biochem Biophys*  
944 183:200–215
- 945 Miura K, Ohgiya S, Hoshino T, Nemoto N, Suetake T, Miura A, Spyrapoulos L, Kondo H, Tsuda  
946 S (2001) NMR analysis of Type III antifreeze protein intramolecular dimer. Structural basis for  
947 enhanced activity. *J Biol Chem* 276:1304–1310
- 948 Mok Y-F, Lin F-H, Graham LA, Celik Y, Braslavsky I, Davies PL (2010) Structural basis for the  
949 superior activity of the large isoform of snow flea antifreeze protein. *Biochemistry*  
950 49:2593–2603
- 951 Neven LG, Duman JG, Beals JM, Castellino FJ (1986) Overwintering adaptations of the stag beetle,  
952 *Ceruchus piceus*: removal of ice nucleators in winter to promote supercooling. *J Comp Physiol*  
953 B 156:707–716
- 954 Neven L, Duman JG, Low MG, Sehl LC, Castellino FJ (1989) Purification and characterization of  
955 an insect hemolymph lipoprotein ice nucleator: evidence for the importance of  
956 phosphatidylinositol and apolipoprotein in the ice nucleator activity. *J Comp Physiol B*  
957 159:71–82
- 958 Nishimiya Y, Ohgiya S, Tsuda S (2003) Artificial multimers of the type III antifreeze protein.  
959 Effects on thermal hysteresis and ice crystal morphology. *J Biol Chem* 278:32307–32312

- Nishimiya Y, Sato R, Takamichi M, Miura A, Tsuda S (2005) Co-operative effect of the isoforms of type III antifreeze protein expressed in Notched-fin eelpout, *Zoarces elongatus* Kner. FEBS J 272:482–492 960
- Olsen TM, Duman JG (1997a) Maintenance of the supercooled state in overwintering pyrochroid beetle larvae, *Dendroides canadensis*: role of hemolymph ice nucleators and antifreeze proteins. J Comp Physiol B 167:105–113 963
- Olsen TM, Duman JG (1997b) Maintenance of the supercooled state in the gut fluid of overwintering pyrochroid beetle larvae, *Dendroides canadensis*: role of ice nucleators and antifreeze proteins. J Comp Physiol B 167:114–122 966
- Olsen TM, Sass SJ, Li N, Duman JG (1998) Factors contributing to seasonal increases in inoculative freezing resistance in overwintering fire-colored beetle larvae *Dendroides canadensis* (Pyrochroidae). J Exp Biol 201:1585–1594 969
- Pertaya N, Marshall CB, DiPrinzio CL, Wilen L, Thomson ES, Wettlaufer JS, Davies PL, Braslavsky I (2007) Fluorescence microscopy evidence for quasi-permanent attachment of antifreeze proteins to ice surfaces. Biophys J 92:3663–3673 972
- Pertaya N, Marshall CB, Celik Y, Davies PL, Braslavsky I (2008) Direct visualization of spruce budworm antifreeze protein interacting with ice crystals: basal plane affinity confers hyperactivity. Biophys J 95:333–341 975
- Poynting JH (1881) Change of state: solid–liquid. Philos Mag 5th series 12:32–48 978
- Ramsay JA (1964) The rectal complex of the mealworm *Tenebrio molitor* L. (Coleoptera, Tenebrionidae). Philos Trans R Soc B 348:279–314 979
- Raymond JA, DeVries AL (1977) Adsorption inhibition as a mechanism of freezing resistance in polar fishes. Proc Natl Acad Sci 74:2589–2593 981
- Reynolds JA, Gilbert DB, Tanford C (1974) Empirical correlation between hydrophobic free energy and aqueous cavity surface area. Proc Natl Acad Sci 71:2925–2927 982
- Schrag JD, O’Grady SM, DeVries AL (1982) Relationship of amino acid composition and molecular weight of antifreeze glycopeptides to non-colligative freezing point depression. Biochim Biophys Acta 717:322–326 983
- Sönnichsen FD, DeLuca CI, Davies PL, Sykes BD (1996) Refined solution structure of type III antifreeze protein: hydrophobic groups may be involved in the energetics of the protein-ice interaction. Structure 4:1325–1337 984
- Sørensen TF, Ramløv H (2001) Variations in antifreeze activity and serum inorganic ions in the eelpout *Zoarces viviparus*: antifreeze activity in the embryonic state. Comp Biochem Physiol A 30:123–132 985
- Stevens CA, Drori R, Zalis S, Braslavsky I, Davies PL (2015) Dendrimer-linked antifreeze proteins have superior activity and thermal recovery. Bioconjug Chem 26:1908–1915 986
- Thomson W (1871) On the equilibrium of vapour at a curved surface of liquid. Philos Mag 42:448–452 987
- Tolls J, van Dijk J, Verbruggen EJM, Hermens JLM, Loeprucht B, Schüürmann G (2002) Aqueous solubility-molecular size relationships: a mechanistic case study using C10- to C19-alkanes. J Phys Chem A 106:2760–2765 988
- Turnbull D (1950) Kinetics of heterogenous nucleation. J Chem Phys 18:198–203 989
- Uhlig HH (1937) The solubilities of gases and surface tension. J Phys Chem 41:1215–1225 990
- Wang L, Duman JG (2005) Antifreeze proteins of the beetle *Dendroides canadensis* enhance one another’s activities. Biochemistry 44:10305–10312 991
- Wang L, Duman JG (2006) A thaumatin-like protein from larvae of the beetle *Dendroides canadensis* enhances the activity of antifreeze proteins. Biochemistry 45:1278–1284 992
- Wang S, Amornwittawat N, Banatiao J, Chung M, Kao Y, Wen X (2009a) Hofmeister effects of common monovalent salts on the beetle antifreeze protein activity. J Phys Chem B 113:13891–13894 993
- Wang S, Amornwittawat N, Juwita V, Kao Y, Duman JG, Pascal TA, Goddard WA, Wen X (2009b) Arginine, a key residue for the enhancing ability of an antifreeze protein of the beetle *Dendroides canadensis*. Biochemistry 48:9696–9703 994

- 1013 Washburn EW (1929) International critical tables of numerical data, physics, chemistry and  
1014 technology, vol 4. McGraw-Hill, New York
- 1015 Wen D, Laursen RA (1992) A model for binding of an antifreeze polypeptide to ice. *Biophys J*  
1016 63:1659–1662
- 1017 Wen X, Wang S, Amornwittawat N, Houghton EA, Sacco MA (2011) Interaction of reduced  
1018 nicotinamide adenine dinucleotide with an antifreeze protein from *Dendroides canadensis*:  
1019 mechanistic implication of antifreeze activity enhancement. *J Mol Recognit* 24:1025–1032
- 1020 Westh HP, Ramløv H, Wilson PW, DeVries AL (1997) Vapor pressure of aqueous antifreeze  
1021 glycopeptide solutions. *Cryo-Letters* 18:277–282
- 1022 Wilson PW (1993) Explaining thermal hysteresis by the Kelvin effect. *Cryo-Letters* 14:31–36
- 1023 Wilson PW, Beaglehole D, DeVries AL (1993) Antifreeze glycopeptide adsorption on single crystal  
1024 ice surfaces using ellipsometry. *Biophys J* 64:1878–1884
- 1025 Wöhrmann APA (1996) Antifreeze glycopeptides and peptides in Antarctic fish species from the  
1026 Weddell Sea and the Lazarev Sea. *Mar Ecol Prog Ser* 130:47–59
- 1027 Wu DW, Duman JG (1991) Activation of antifreeze proteins from larvae of the beetle *Dendroides*  
1028 *canadensis*. *J Comp Physiol B* 161:279–283
- 1029 Wu DW, Duman JG, Xu L (1991) Enhancement of antifreeze protein activity by antibodies.  
1030 *Biochim Biophys Acta* 1076:416–420
- 1031 Xu H, Griffith M, Patten CL, Glick BR (1998) Isolation and characterization of an antifreeze protein  
1032 with ice nucleation activity from the plant growth promoting rhizobacterium *Pseudomonas*  
1033 *putida* GR12-2. *Can J Microbiol* 44:64–73
- 1034 Yang DSC, Sax M, Chakrabarty A, Hew CL (1988) Crystal structure of an antifreeze polypeptide  
1035 and its mechanistic implications. *Nature* 333:232–237
- 1036 Yeung KL, Wolf EE, Duman JG (1991) A scanning tunneling microscopy study of an insect  
1037 lipoprotein ice nucleator. *J Vac Sci Technol B* 9:1197–1201
- 1038 Zachariassen KE, Hammel HT (1976) Nucleating agents in the haemolymph of insects tolerant to  
1039 freezing. *Nature* 262:285–287
- 1040 Zachariassen KE, Husby JA (1982) Antifreeze effect of thermal hysteresis agents protects highly  
1041 supercooled insects. *Nature* 298:865–867
- 1042 Zachariassen KE, DeVries AL, Hunt B, Kristiansen E (2002) Effect of ice fraction and dilution  
1043 factor on the antifreeze activity in the hemolymph of the cerambycid beetle *Rhagium inquisitor*.  
1044 *Cryobiology* 44:132–141
- 1045 Zanetti-Polzi L, Biswas AD, Del Galdo S, Barone V, Daidone I (2019) Hydration shell of antifreeze  
1046 proteins: unveiling the role of non-ice-binding surfaces. *J Phys Chem B* 123:6474–6480
- 1047 Zepeda S, Yokoyama E, Uda Y, Katagiri C, Furukawa Y (2008) *In situ* observation of antifreeze  
1048 glycoprotein kinetics at the ice interface reveals a two-step reversible adsorption mechanism.  
1049 *Cryst Growth Des* 8:3666–3672

# Author Query

Chapter No.: 6	385597_1_En
----------------	-------------

---

Query Refs.	Details Required	Author's response
AU1	Please check and confirm the edit made in the sentence beginning "Such perpetual motion of water molecules would..."	

Uncorrected Proof